Blue-Noise Sampling of Signals on Graphs

1st Alejandro Parada-Mayorga
University of Delaware
Newark, DE, USA
alejopm@udel.edu

2nd Daniel L. Lau
University of Kentucky
Lexington, Kentucky, USA
dllau@uky.edu

3rd Jhony H. Giraldo
University of Delaware
Newark, DE, USA
jgiraldo@udel.edu

4th Gonzalo R. Arce
University of Delaware
Newark, DE, USA
arce@udel.edu

***Abstract*—In this work we introduce the concept of blue noise sampling, traditionally used in imaging applications, for bandlimited signals on graphs. We show how the spectral and vertex domain characterization of these patterns is connected with results about the quality of the sampling sets already existing in the literature. We provide numerical evidence that shows that these patterns are also competitive with respect to the state of the art sampling techniques in terms of the reconstruction error.**

I. Introduction

The interest on data processing grows every year, requiring new insights about how to handle large datasets defined on nonlinear and/or irregular structures. Emerging fields such as geometric deep learning and graph signal processing put in a central scenario the analysis of signals on manifolds and graphs, and efforts are made to generalize tools that are key in traditional signal processing to these new areas [1] [2].

Following this trend we introduce blue noise sampling on graphs, showing how part of the benefits that are obtained from blue noise in traditional halftoning [3] and imaging are also attainable for signals on graphs. These blue noise sampling patterns are characterized by a low frequency energy on the spectral domain and a homogeneous distribution of the sampling nodes that are located as far as possible from each other. The connection between blue noise and sampling sets on graphs is established, rooted and inspired by the work of Pesenson on manifolds [4], [5] and graphs [6]–[8]. Additionally, simulations are performed in order to test blue noise sampling sets against the state of the art sampling techniques.

This paper is organized as follows. In Section II notation and preliminaries about sampling on graphs will be discussed, whereas in Section III the concept of blue noise sampling on graphs will be discussed. In Section IV an algorithm for the generation of blue noise on graphs is presented. Section V provides numerical simulations where blue noise is tested against the state of the art techniques and finally in Section VI conclusions are provided.

II. Sampling Theory on Graphs

When functions (signals) are considered on Euclidean domains the question of whether a sampling pattern provides uniqueness for the representation of the function has been answered fairly well [1], but this question remained partially open on more general spaces like manifolds until the work presented in [4], [5], where it was stated how the characteristics of the sampling pattern on the manifold determined the error in the reconstruction, when the function was represented as a linear combination of eigenfunctions of the Laplace-Beltrami operator [4], [9]. In particular it was established that when open balls of the same radius are centered around the sampling points, the minimum radius should be selected such that they form a cover of the manifold, and this radius is directly related to the quality of the reconstruction of the function from those sampling points. In the halftoning community, these kind of patterns are called *blue noise* type because of their characteristics on the Fourier domain, where the energy is concentrated around high frequencies [3], [10].

In a variety of applications graphs are used as discrete representations of manifolds when concrete calculations are required [2], and therefore an extension of the results obtained in [4], [5] was desirable. Pesenson established analogs of those results in [6]–[8] introducing new concepts and parameters that provide a measure of the quality of a sampling set of nodes, indicating weather the values of a bandlimited signal on those nodes provide a unique representation of the whole signal itself. In the sections below a connection between those quantities and blue noise sampling patterns is established.

A. Background and notation

Let $G = (\mathcal{V}, \mathcal{E})$ be a weighted graph with vertex set $\mathcal{V}$, and edges set, $\mathcal{E}$. $\mathbf{W}$ is the adjacency matrix, with $\mathbf{W}(u, v)$ being the weight connecting the nodes u and v. $\mathbf{D}$ is the diagonal matrix with entries given by $\mathbf{D}(u, u) = \sum_{v \neq u} \mathbf{W}(v, u)$. The Laplacian matrix is defined as $\mathbf{L} = \mathbf{D} - \mathbf{W}$, and its eigenvalues are given by $0 \leq \mu_1 \leq \mu_2 \leq \ldots \leq \mu_N$, $N = |\mathcal{V}|$ [1]. The path between two nodes v_1 and v_n is represented by the sequence of nodes $(v_1, v_2, \ldots, v_{n-1}, v_n)$, with $\mathbf{W}(v_i, v_{i+1}) \neq 0$ for $1 \leq i \leq n-1$; and its length is given by

$$|(v_1, v_2, \ldots, v_{n-1}, v_n)| = \sum_{i=1}^{n-1} \mathbf{W}(v_i, v_{i+1}). \tag{1}$$

The path between the nodes u and v with the shortest length is denoted by $\gamma_{u,v}$. In what follows we will refer to $|\gamma_{u,v}|$ as the geodesic distance between the nodes u and v. The matrix of geodesic distances between nodes is denoted by $\mathbf{\Gamma}$, where $\mathbf{\Gamma}(u, v) = |\gamma_{u,v}|$.

A signal, $\boldsymbol{x}$, on the graph is then defined as the map $\boldsymbol{x} : \mathcal{V} \longrightarrow \mathbb{R}$ represented by the vector $\boldsymbol{x} \in \mathbb{R}^N$ where $\boldsymbol{x}(v)$ is the value of the signal on $v \in \mathcal{V}$.

The spectral decomposition of $\mathbf{L}$ is indicated as $\mathbf{L} = \mathbf{U}\mathbf{\Lambda}\mathbf{U}^\mathsf{T}$, where $\mathbf{U}$ is the matrix of eigenvectors. The Graph Fourier Transform of the signal, $\boldsymbol{x}$, is given by $\hat{\boldsymbol{x}} = \mathbf{U}^\mathsf{T}\boldsymbol{x}$ and $\boldsymbol{x} = \mathbf{U}\hat{\boldsymbol{x}}$. We say that the signal $\boldsymbol{x}$ has bandwidth ω on the spectral axes, if $\boldsymbol{x}(k) = 0$ for all $\mu_k > \omega$, on the discrete axes the bandwidth is given by k. The set of signals of bandwidth ω is represented as $PW_\omega(G) = \text{span}\{\mathbf{U}_k : \mu_k \leq \omega\}$ which is the so called Paley-Wiener space of bandwidth ω [7], where $\mathbf{U}_k$ represents the first k column vectors of $\mathbf{U}$. The sampled version of the signal $\boldsymbol{x}$ on $\mathcal{S} \subset \mathcal{V}$ is given by $\boldsymbol{x}_\mathcal{S} = \mathbf{M}\boldsymbol{x}$ where $\mathbf{M} = [\boldsymbol{\delta}_{s_1}, \ldots, \boldsymbol{\delta}_{s_m}]^\mathsf{T}$, $s_i \in \mathcal{S}\ \forall\ i = 1, \ldots, m$ and $\boldsymbol{\delta}_v$ is the Kronecker column vector centered at $v \in \mathcal{V}$. If $\boldsymbol{x}$ is bandlimited, it can be reconstructed from $\boldsymbol{x}_\mathcal{S}$ as:

$$\boldsymbol{x}_{rec} = \underset{\boldsymbol{z} \in span(\mathbf{U}_k)}{\text{argmin}} \|\mathbf{M}\boldsymbol{z} - \boldsymbol{x}_\mathcal{S}\|_2^2 = \mathbf{U}_k \left(\mathbf{M}\mathbf{U}_k\right)^\dagger \boldsymbol{x}_\mathcal{S} \quad (2)$$

where $(\mathbf{M}\mathbf{U}_k)^\dagger$ is the pseudo-inverse of $\mathbf{M}\mathbf{U}_k$ [11]. When the reconstruction of the signal is performed, the desired sampling set should be the one that minimizes the error in (2). In what follows, we will refer to the ratio between the number of sampling nodes and the total number of nodes as the density $d = m/N$ of the sampling. A theoretical characterization of the sampling sets was proposed in [7], [8] using the concept of removable sets. In particular, a Λ-removable set for $\Lambda > 0$ is the subset, $\mathcal{S} \subset \mathcal{V}$, for which: $\|\boldsymbol{x}\|_2 \leq (1/\Lambda)\|\mathbf{L}\boldsymbol{x}\|_2\ \forall\ \boldsymbol{x} \in L_2(\mathcal{S})$, where $L_2(\mathcal{S})$ is the set of all functions on $\mathcal{V}$, with support in $\mathcal{S} \subset \mathcal{V}$ and finite ℓ_p norm. The best value of the constant, calculated as $\inf_\Lambda(1/\Lambda)$, is denoted by $\Lambda_\mathcal{S}$. Considering this concept Pesenson states conditions under which the sampling set for a bandlimited signal determines in a unique way the signal in $\mathcal{V}$, using the following theorem:

Theorem 1 (Theorem 5.1 in [7])
If for a set $\mathcal{U} \subset \mathcal{V}$, its compliment $\mathcal{U}^c = \mathcal{V} \setminus \mathcal{U}$ is a $\Lambda_{\mathcal{U}^c}-$removable set, then all signals in $PW_\omega(G)$ are completely determined by its values in $\mathcal{U}$, whenever $0 < \omega < \Lambda_{\mathcal{U}^c}$.

Theorem 1 provide a way to measure the quality of any sampling set. It can be said that the best sampling sets are the ones that lead to the maximum values of $\Lambda_{\mathcal{S}^c}$. In the following sections a result stated in [12] will be presented, in which it is indicated how blue noise sampling patterns indeed promote large values of $\Lambda_{\mathcal{S}^c}$.

B. Previous sampling approaches

There are very well known methods that build the sampling set with greedy algorithms that depend on spectral decompositions of the operators involved. In particular, Chen [13] proposes to find the optimal sampling set, as $\mathcal{S}^{opt} = \arg\max_{|\mathcal{S}|=m} \sigma_1^2$, on the other hand in [14] the optimal set is obtained as $\mathcal{S}^{opt} = \arg\max_{|\mathcal{S}|=m} \sum_{i=1}^k \sigma_i^{-2}$ and in [11] $\mathcal{S}^{opt} = \arg\max_{|\mathcal{S}|=m} \prod_{i=1}^k \sigma_i^2$; with σ_i being i^{th} singular value of $\mathbf{M}\mathbf{U}_k$. In [14] *graph spectral proxies* of order q, $\Omega_q(\mathcal{S}) = (\sigma_{1,q})^{\frac{1}{2q}}$, are introduced to reduce the computational cost for the calculation of the optimal sampling set, where $\sigma_{1,q}$ is the smallest eigenvalue of $(\mathbf{L}^\mathsf{T}_{\mathcal{S}^c,\mathcal{S}^c})^q \mathbf{L}^q_{\mathcal{S}^c,\mathcal{S}^c}$, with $\mathbf{L}^q$ being the q^{th} power of $\mathbf{L}$ and $\mathbf{L}_{\mathcal{S}^c,\mathcal{S}^c}$ the matrix obtained removing the rows and columns of $\mathbf{L}$ indexed by $\mathcal{S}$. It is shown in [14] that for any q and any $\mathcal{S} \subset \mathcal{V}$, zero error reconstruction is achieved when $\omega < \Omega_q(\mathcal{S})$. The optimal sampling set is then given by

$$\mathcal{S}^{opt} = \arg \max_{|\mathcal{S}|=m} \Omega_q(\mathcal{S}). \quad (3)$$

In order to solve (3) a heuristic rule is proposed based on a spectral decomposition, adding one node at a time. A node is added to the sampling set following the index location of the component with the highest absolute value for the first eigenvector of $\mathbf{L}^q_{\mathcal{S}^c,\mathcal{S}^c}$ with $\mathcal{S}$ being the previous sampling set. The quality of the sampling set increases as the value of q is increased, but large values of q lead to a higher computational cost. In some cases eigenvalue decompositions are not available, and therefore techniques like the ones presented above are not applicable. Puy [15] proposes an approach in which the nodes are selected according to a random matrix $\mathbf{P}$ that is designed jointly with $\mathbf{M}$ and the reconstruction of the sampled signal is obtained from

$$\boldsymbol{x}_{rec} = \arg \min_{\boldsymbol{z} \in \mathbb{R}^N} \left(\left\| \mathbf{P}^{-1/2}(\mathbf{M}\boldsymbol{z} - \boldsymbol{x}_\mathcal{S}) \right\|_2^2 + \tau \boldsymbol{z}^\intercal g(\mathbf{L}) \boldsymbol{z} \right), \quad (4)$$

where $\tau \in \mathbb{R}^+$ and g is a single variable polynomial. Both, τ and g, are selected empirically. The selection of the entries of $\mathbf{P}$ requires the spectral decomposition of $\mathbf{L}$, however Puy [15] proposes an eigen decomposition free calculation of $\mathbf{P}$ that leads to an approximate solution of (4), and it is proven that $\mathbf{M}\mathbf{P}^{-1/2}$ satisfies the restricted isometry property for a number of samples in the order of $O(k \log k)$. In [11] Tremblay uses *determinantal point processes (DPP)* for the estimation of $\mathbf{P}$ in Puy's approach including the cases where eigen decompositions are not available. In [16] and [17] similar vertex-domain sampling methods are proposed relying on the properties of the so called *localization operator* introduced in [18]. In those approaches the sampling set is built using a greedy algorithm that evaluates a cost function that can be calculated using Chebyshev polynomial approximations, avoiding the use of any spectral decomposition. The cost function is designed to avoid overlapping between the localization operators centered at the sampling nodes. These approaches have some similarities with the approach we propose in this paper, however the generation of the patterns and the theoretical insights about their nature differ substantially. In particular we show, how blue noise sampling patterns are characterized by a low redness which is something desirable in order to increase

In [19] the sampling of signals on graphs is considered in those scenarios in which the information from one single node is available for different orders of the shifting operator.

III. Blue Noise Sampling on Graphs

Blue noise sampling has been extensively used in applications related to the representation and printing of images, where a gray scale picture has to be represented with a binary

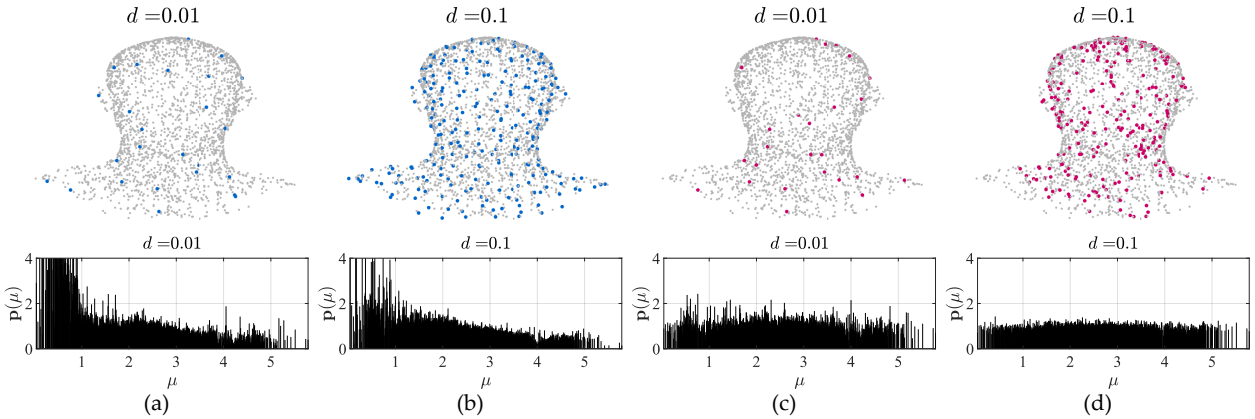

Fig. 1. Different sampling patterns on a graph displaying the nodes distribution in the three dimensional space for a density sampling of $d = 0.01$ and $d = 0.1$ and their power spectrums. (a)-(b): Blue noise sampling patterns. (c)-(d): Random sampling patterns

pattern that should be able to preserve the properties of the original image that are most important to the human eye. More specifically this representation is desired to be free of artifacts and it should be representative of the gray scale tones of the original image [3]. The spatial characteristics of these blue noise sampling patterns and its typical Fourier spectrum allows their generation. Following these same principles we describe the expected characteristics of blue noise on graphs.

A. Fourier Statistics

The Fourier spectrum of averaged blue noise sampling patterns is characterized for a low energy content in the low frequencies [3]. With the purpose of quantifying the power spectrum of a family of sampling patterns on a graph we propose to average the spectrum of several realizations of these patterns. Then, if q is the number of realizations, $\boldsymbol{x}_1, \boldsymbol{x}_2, \ldots, \boldsymbol{x}_q$, of a stochastic signal, its power spectrum can be defined as $\mathbf{p}(\ell) = \frac{N}{q}\sum_{i=1}^{q}\frac{\hat{\boldsymbol{x}}_i(\ell)^2}{\|\hat{\boldsymbol{x}}_i\|_2^2} \quad \ell = 2, \ldots, N$; where the ℓ^{th} component of $\mathbf{p}$ is associated to the ℓ^{th} Fourier coefficient. If the families of patterns are completely random, the shape of $\mathbf{p}(\ell)$ is expected to be flat. Fig. 1 illustrates the power spectrum of random and blue noise sampling patterns depicting also a realization of the vertex-domain characteristics of the patterns being used. Then, approximate versions of blue noise sampling patterns can be defined as the minimizers of $R_{\boldsymbol{s}}$, as

$$R_{\boldsymbol{s}} = \frac{1}{m}\sum_{\ell=2}^{N}\frac{\hat{\boldsymbol{s}}(\ell)^2}{\mu_\ell}, \tag{5}$$

where $\boldsymbol{s} \in \{0,1\}^N$ is the characteristic function of the sampling set. Notice that in $R_{\boldsymbol{s}}$ the low frequency content is penalized.

B. Spatial characteristics of Blue-Noise

Fig. 1 shows the vertex distribution of the sampling nodes, expected from a blue noise sampling pattern. As can be appreciated there is a *spread uniformity* between sampling nodes, in the sense that they are located as far as possible from each other. This property is going to be used in the following section for the systematic generation of blue noise sampling patterns.

C. Blue-noise Sampling Sets

In Theorem 1, it was stated that the sampling sets, $\mathcal{S}$, should lead to the largest possible values of $\Lambda_{\mathcal{S}^c}$ for high quality reconstructions. The following theorem, presented in [12] establishes the relationship between the blue noise cost function $R_{\boldsymbol{s}}$ and $\Lambda_{\mathcal{S}^c}$.

Theorem 2 (Theorem 8, [12])
Let $\boldsymbol{s} : \mathcal{V} \longrightarrow \{0,1\}$ be a sampling pattern with $\boldsymbol{s}|_{\mathcal{S}} = 1$, $\boldsymbol{s}|_{\mathcal{S}^c} = 0$ for $\mathcal{S} \subset \mathcal{V}$ and $|\mathcal{S}| = \|\boldsymbol{s}\|_0 = m$, then the $\Lambda_{\mathcal{S}^c}-$constant of the set $\mathcal{S}^c$ satisfies

$$\Lambda_{\mathcal{S}^c} > C_\delta \left(\frac{R_{\boldsymbol{s}}}{vol(G)R_{\boldsymbol{s}} - m\left(1 - \frac{m}{N}\right)^2} \right)^{\frac{2}{\delta}} \tag{6}$$

where $vol(G) = \sum_{v=1}^{N}\mathbf{D}(v,v)$; δ is the isoperimetric dimension of G [6]; and C_δ a constant that depends only on δ.

from this theorem, we can appreciate that blue noise sampling on graphs promotes large values of $\Lambda_{\mathcal{S}^c}$. In the following sections we present an algorithm for the generation of these patterns.

IV. Generating Blue-Noise Sampling Sets

Exploiting the vertex-domain characteristics of blue noise sampling patterns, we propose an algorithm inspired in the so called *void and cluster* algorithm [20] used in digital halftoning for the generation of blue noise sampling patterns. The proposed algorithm works relocating a set of initial sampling nodes, determining regions where there is low and high density of sampling nodes, respectively. Then, some of the nodes in those high density regions are relocated in the low density ones. The details of the proposed scheme can be appreciated in Algorithm 1, where the geodesic distances between sampling nodes are maximized, filling void-like regions and reducing clustered-like regions in the vertex domain of the graph. The location of the sampling nodes is achieved

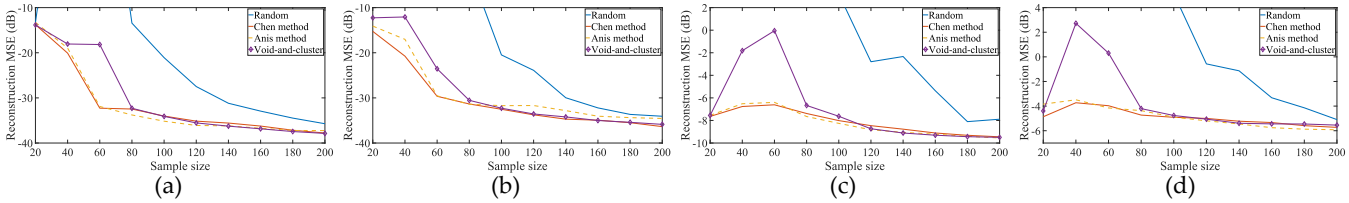

Fig. 2. The averaged mean squared error of the reconstructed signals from a sampled representation: (a) The graph G_1 and the signal model SM1. (b) The graph G_2 and the signal model SM1. (c) The graph G_1 and the signal model SM2. (d) The graph G_2 and the signal model SM2.

using the geodesic distances on the graph, $\mathbf{\Gamma}$, mapped on a gaussian kernel $\mathbf{K}(i,j) = e^{-\frac{\mathbf{\Gamma}(i,j)^2}{\sigma}}$, where σ is related with the average distance between sampling points. The distances between sampling points are computed iteratively in $\mathbf{c}$, and the support of the sampling pattern is used to update the components of $\mathbf{c}$. The use of $\mathbf{K}$ promotes emphasis on the local information surrounding a sampling node. Algorithm 1 can be synthesized in two big steps. In the first step, we calculate the distances between sampling nodes via $\mathbf{K}$ and we storage those values as $\mathbf{c}(\text{supp}(\boldsymbol{s})) = \sum \mathbf{K}(\text{supp}(\boldsymbol{s}), \text{supp}(\boldsymbol{s}))$, then if $\boldsymbol{s}(v) = 1$ the value of $\mathbf{c}(v)$ is the sum of the distance between v and all the other sampling nodes. The component of $\mathbf{c}$ with the maximum value corresponds to the sampling node that is *closest* to the other sampling nodes and will be typically located at the center of a *cluster*. In the second step of the algorithm we calculate the distances between the sampling nodes and all the nodes u where $\boldsymbol{s}(u) = 0$, and those values are kept as $\mathbf{c}(\text{supp}(\boldsymbol{s})^c) = \sum \mathbf{K}(\text{supp}(\boldsymbol{s}), \text{supp}(\boldsymbol{s})^c) - \tau$ where τ is selected to guarantee that $\mathbf{c}(\text{supp}(\boldsymbol{s})^c)$ is always negative. Several values of τ can be selected, in this work we chose $\tau \geq N$. The component associated to the minimum value of $\mathbf{c}$ is associated to the largest *void* on $V(G)$.

Algorithm 1 Void and cluster algorithm for graphs

Input: m: number of samples, σ.
Output: $\boldsymbol{s}$: sampling pattern
Initialisation : $\boldsymbol{s} = \mathbf{0}$, `IndA=-1`, `IndB=-1`.
Calculate $\mathbf{K}(i,j) = e^{-\frac{\mathbf{\Gamma}(i,j)^2}{\sigma}}$ for all $1 \leq i,j \leq N$.
$\mathbf{c} = \mathbf{K}\mathbf{1}_{N\times 1}$.
Get $\mathcal{M}$ as m random nodes on $\mathcal{V}$.
$\boldsymbol{s}(\mathcal{M}) = 1$.
for $r = 1:1:N$ **do**
  $\mathbf{c}(\text{supp}(\boldsymbol{s})) = \sum \mathbf{K}(\text{supp}(\boldsymbol{s}), \text{supp}(\boldsymbol{s}))$.
  $\mathbf{c}(\text{supp}(\boldsymbol{s})^c) = \sum \mathbf{K}(\text{supp}(\boldsymbol{s}), \text{supp}(\boldsymbol{s})^c) - \tau$.
  $\boldsymbol{s}(\arg\max_i\{\mathbf{c}(i)\}) = 0$.
  $\boldsymbol{s}(\arg\min_i\{\mathbf{c}(i)\}) = 1$.
  if `IndA`=$\arg\max_i\{\mathbf{c}(i)\}$ and `IndB`=$\arg\min_i\{\mathbf{c}(i)\}$ **then**
    break
  else
    `IndA`=$\arg\min_i\{\mathbf{c}(i)\}$.
    `IndB`=$\arg\max_i\{\mathbf{c}(i)\}$.
  end if
end for
return $\boldsymbol{s}$

Then, repeating these two steps iteratively a blue noise sampling pattern is obtained. The vertex-domain characteristics of a blue noise sampling pattern can be appreciated in Fig. 1 where several sampling densities are considered. The vertex domain spreading and the uniformity of the generated blue noise patterns are evident in contrast with randomly generated patterns.

V. Experiments

In order to test blue noise sampling patterns against other state of the art techniques, we performed a numerical experiment in which two graph models are considered. For each graph, 100 signals are generated, sampled and then reconstructed for different sampling rates, where the reconstruction is performed by means of eqn. (2). The mean squared error (MSE) is calculated for each reconstructed signal and then averaged by 100.

The sampling schemes are: random sampling, blue noise by void and cluster, Chen's scheme [13] and Anis's approach [14]. We consider two signal models: SM1, in which a random signal of bandwidth $k = 50$ is generated choosing the Fourier coefficients from the Gaussian distribution $\mathcal{N}(0, 0.5^2)$ and the samples captured are contaminated with Gaussian additive noise keeping the signal to noise ratio as $SNR = 20$dB, and signal model SM2 where a random signal is generated with the Gaussian distribution $\mathcal{N}(0, 0.5^2)$ and its coefficients are modulated by the function $h(\mu)$

$$h(\mu) = \begin{cases} 1 & \text{If} \quad \mu \leq \mu_{50} \\ e^{-4(\mu-\mu_{50})} & \text{If} \quad \mu > \mu_{50} \end{cases} \tag{7}$$

For the experiment a Swiss roll graph G_1 with $N = 1000$ nodes and a sensor network graph G_2 with $N = 600$ nodes are considered.

Fig. 2 illustrates the reconstruction error of different signals from a set of samples considering several sampling rates. The results show consistently that blue noise sampling leads to comparable results with respect to the state of the art methods.

VI. Conclusion

In this paper blue noise sampling was introduced for the sampling of signals on graphs. The results obtained in terms of the reconstruction error are competitive against the state of the art techniques. The generation of these patterns follows the intuitive principle of spreading the sampling nodes as far as possible from each other, which is a reasonable consideration in most cases because if the sampling nodes are too close to each other the whole signal would not be properly characterized or uniquely determined by its samples.

REFERENCES

[1] D. I. Shuman, S. K. Narang, P. Frossard, A. Ortega, and P. Vandergheynst. The emerging field of signal processing on graphs: Extending high-dimensional data analysis to networks and other irregular domains. *IEEE Signal Processing Magazine*, 30(3):83–98, May 2013.

[2] M. M. Bronstein, J. Bruna, Y. LeCun, A. Szlam, and P. Vandergheynst. Geometric deep learning: Going beyond euclidean data. *IEEE Signal Processing Magazine*, 34(4):18–42, July 2017.

[3] R. A. Ulichney. Dithering with blue noise. *Proceedings of the IEEE*, 76(1):56–79, 1988.

[4] Isaac Z. Pesenson. A sampling theorem on homogeneous manifolds. *Trans. Amer. Math.*, 352:4257–4269, April 2000.

[5] Isaac Pesenson. Poincaré-type inequalities and reconstruction of paley-wiener functions on manifolds. *The Journal of Geometric Analysis*, 14(1):101–121, Mar 2004.

[6] Hartmut Fuhr and Isaac Z. Pesenson. Poincar and plancherel polya inequalities in harmonic analysis on weighted combinatorial graphs. *SIAM Journal on Discrete Mathematics*, 27(4):2007–2028, 2013.

[7] I. Z. Pesenson. Sampling solutions of schrodinger equations on combinatorial graphs. In *2015 International Conference on Sampling Theory and Applications (SampTA)*, pages 82–85, May 2015.

[8] Isaac Z. Pesenson and Meyer Z. Pesenson. Sampling filtering and sparse approximations on combinatorial graphs. *Journal of Fourier Analysis and Applications*, 16(6):921–942, Dec 2010.

[9] I. Z. Pesenson. Sampling and weyl's law on compact riemannian manifolds. In *2017 International Conference on Sampling Theory and Applications (SampTA)*, pages 92–95, July 2017.

[10] D. Lau, R. Ulichney, and G. R. Arce. Blue and green noise halftoning models. *IEEE Signal Processing Magazine*, 2(4):28–38, 2003.

[11] Nicolas Tremblay, Pierre-Olivier Amblard, and Simon Barthelmé. Graph sampling with determinantal processes. *CoRR*, abs/1703.01594, 2017.

[12] A. Parada-Mayorga, D.L. Lau, J. Giraldo, and G. . Arce. Blue-Noise Sampling on Graphs. *ArXiv e-prints*, December 2018.

[13] S. Chen, R. Varma, A. Sandryhaila, and J. Kovaevi. Discrete signal processing on graphs: Sampling theory. *IEEE Transactions on Signal Processing*, 63(24):6510–6523, Dec 2015.

[14] A. Anis, A. Gadde, and A. Ortega. Efficient sampling set selection for bandlimited graph signals using graph spectral proxies. *IEEE Transactions on Signal Processing*, 64(14):3775–3789, July 2016.

[15] Gilles Puy, Nicolas Tremblay, Rmi Gribonval, and Pierre Vandergheynst. Random sampling of bandlimited signals on graphs. *Applied and Computational Harmonic Analysis*, 44(2):446 – 475, 2018.

[16] A. Jayawant and A. Ortega. A distance-based formulation for sampling signals on graphs. In *2018 IEEE International Conference on Acoustics, Speech and Signal Processing (ICASSP)*, pages 6318–6322, April 2018.

[17] A. Sakiyama, Y. Tanaka, T. Tanaka, and A. Ortega. Eigendecomposition-free sampling set selection for graph signals. *IEEE Transactions on Signal Processing*, 67(10):2679–2692, May 2019.

[18] D. I. Shuman, P. Vandergheynst, D. Kressner, and P. Frossard. Distributed signal processing via chebyshev polynomial approximation. *IEEE Transactions on Signal and Information Processing over Networks*, 4(4):736–751, Dec 2018.

[19] A. G. Marques, S. Segarra, G. Leus, and A. Ribeiro. Sampling of graph signals with successive local aggregations. *IEEE Transactions on Signal Processing*, 64(7):1832–1843, April 2016.

[20] Robert A. Ulichney. Void-and-cluster method for dither array generation, 1993.